J Mater Sci (2006) 41:4636–4642
DOI 10.1007/s10853-006-0031-x

Study of lithium–zinc borophosphate glasses

L. Koudelka · J. Jirák · P. Mošner · L. Montagne ·
G. Palavit

Received: 18 April 2005 / Accepted: 16 September 2005 / Published online: 4 May 2006

Abstract Mixed lithium–zinc borophosphate glasses were prepared and studied in three compositional series xLi$_2$O–(50−x)ZnO–50P$_2$O$_5$, xLi$_2$O–(50−x)ZnO–10B$_2$O$_3$–40P$_2$O$_5$ and xLi$_2$O–(50−x)ZnO–20B$_2$O$_3$–30P$_2$O$_5$ with x = 0, 10, 20, 30, 40 and 50 mol% Li$_2$O. The obtained glasses were characterized by the measurements of the density (ρ), molar volume (V_M), glass transition temperature (T_g) and thermal expansion coefficient (α). For the investigation of structural changes ^{11}B and ^{31}P MAS NMR and Raman spectroscopy were applied. The replacement of zinc by lithium in borophosphate glasses slightly decreases V_M and T_g, while α increases. In Li–Zn metaphosphate glasses the compositional dependence of T_g reveals a minimum, while at the borophosphate series T_g decreases monotonously with increasing Li$_2$O content. Chemical stability of Li–Zn borophosphate glasses is very good for glasses with x = 0–30 mol% Li$_2$O. Spectral studies showed in the glass series with 10 mol% B$_2$O$_3$ only the presence of BO$_4$ sites. In the glasses with 20 mol% B$_2$O$_3$ the presence of BO$_3$ and two BO$_4$ sites was revealed in ZnO-rich glasses and only one BO$_4$ site in Li$_2$O-rich glasses; the number of BO$_3$ groups decreases with increasing Li$_2$O content which is ascribed to the formation of P–O–Zn covalent bonds in ZnO-rich glasses.

Introduction

The structure of glasses is determined mostly by the anionic network, whereas the effect of cations is usually smaller. Nevertheless in some cases the formation of glasses with a suitable combination of cations can advantageously affect the properties of glasses. Phosphate and borophosphate glasses of silver and lithium were studied as fast ion conductors [1–3]. Nevertheless, alkali phosphate glasses reveal a high solubility and therefore the modification of their composition by the changes in anionic or cationic part can increase their chemical stability.

The structure of rapidly quenched lithium phosphate glasses xLi$_2$O-(1−x)P$_2$O$_5$ within the concentration range x = 0.5–0.75 was investigated by Tatsumisago et al. [4] using IR and Raman spectroscopy. They found the values of T_g to be almost constant within the studied compositional range and from spectral studies they found that with increasing Li$_2$O content metaphosphate units convert gradually into diphosphate units and then into orthophosphate units. Vitreous electrolytes based on lithium borophosphates were studied by Magistris et al. [5]. The structure of lithium borophosphate glasses was investigated by Raman spectroscopy [6, 7] and ^{31}P MAS NMR spectroscopy [8, 9]. They identified several different types of phosphate units. Beside BPO$_4$-like units they identified PO$_4$ units connected to one boron atom (MB1 units) and to two boron atoms (MB2 units) and one metal atom and also the PO$_4$ units connected to one boron atom and two metal ions (EB units). They proposed that MB2 units are mostly connected with three-coordinated boron, while MB1 units are coordinated to BO$_4$ units.

Zinc borophosphate glasses were studied by Brow and Tallant [10] in the series x(B$_2$O$_3$)-(1−x)Zn(PO$_3$)$_2$ and y(B$_2$O$_3$)-(1−y)ZnP$_2$O$_7$ by ^{31}P and ^{11}B MAS NMR

L. Koudelka (✉) · J. Jirák · P. Mošner
Department of General and Inorganic Chemistry, Faculty of Chemical Technology, University of Pardubice, 532 10 Pardubice, Czech Republic
e-mail: ladislav.koudelka@upce.cz

L. Montagne · G. Palavit
Laboratoire de Cristallochimie et Physicochimie du Solide, Ecole Nationale Superieure de Chimie de Lille, BP108, Villeneuve d'Ascq cedex, 59652, France

spectroscopy, whereas in paper [11] the properties of zinc borophosphate glasses of the system xZnO–yB$_2$O$_3$–zP$_2$O$_5$ were studied in compositional series with 30, 40, 50 and 60 mol% P$_2$O$_5$.

For the glasses derived from metaphosphate composition, the values of the glass transition temperature T_g increase with an increasing B$_2$O$_3$ content and reach a maximum at the glasses containing ~20 mol% B$_2$O$_3$ [10–12]. The observed increase is explained by a transformation of the chain-like structure, characteristic of metaphosphate glasses, into the three-dimensional structure due to the incorporation of boron in the prevailing form of BO$_4$ tetrahedra [12].

This paper is devoted to the study of properties and structure of ZnO–Li$_2$O mixed metaphosphate and borophosphate glasses with 10 and 20 mol% B$_2$O$_3$ in which Li$_2$O replaces ZnO, i.e. one Zn^{2+} cation is replaced by two Li$^+$ ions.

Experimental

Samples of the Li$_2$O–ZnO–B$_2$O$_3$–P$_2$O$_5$ glasses were prepared in the batches of 25 g by the reaction of LiOH · H$_2$O, ZnO, H$_3$BO$_3$ and H$_3$PO$_4$. In the first stage the reaction mixture was heated slowly in a Pt crucible up to 600 °C with the final calcination at the maximum temperature for 2 h to remove water. After the calcination the reaction mixture was heated slowly up to the 850–1220 °C. After 20 min heating at the maximum temperature, the obtained melt was cooled by pouring into a graphite mould of 30 × 30 mm dimensions to form a suitable glass block. The obtained glasses were separately annealed for 15 min at a temperature about their T_g and then slowly cooled to the room temperature. Transformation temperature T_g was obtained from DTA measurements before the annealing.

The glass density, ρ, was determined at bulk samples by the Archimedes method using CCl$_4$ as the immersion liquid. The molar volume V_M was calculated as $V_M = \bar{M}/\rho$, where $\bar{M}$ is the average molar weight of the glass composition wLi$_2$O–xZnO–yB$_2$O$_3$–zP$_2$O$_5$ calculated for $w + x + y + z = 1$. The chemical durability of the glasses was evaluated at room temperature from the measurements of the conductivity of a solution obtained by the interaction of 0.3 g of the glass powder (mean diameter of 8 µm) with 100 mL of distilled water for 60 min.

Thermal expansion coefficient and the glass transition temperature were measured on the equipment TMA CX04R (RMI Pardubice) at the heating rate of 5 K min^{-1}. For the measurement of dilatation curves the cubes with dimensions of 5 × 5 × 5 mm were cut out from the bulk samples. From the obtained curves the coefficient of thermal expansion, α, was determined as a mean value in the temperature range of 150–250 °C. The glass transition temperature, T_g, was determined from the change in the slope of the elongation versus temperature plot. Thermal behaviour of the glasses was studied with the Perkin Elmer DTA-DSC equipment, model 1700, working in the temperature range of 50–800 °C at a scan rate of 10 °C min^{-1} in the DSC mode. The measurement was done on powder samples with mean diameter 8–10 µm placed in sealed vacuum silica ampoules.

The Raman spectra were measured on bulk samples at room temperature on a FT IR spectrometer, Bruker model IFS 55, with the Raman attachment, FRA 106. The Raman spectra were recorded under excitation with a Nd:YAG laser radiation using a slit width of 4 cm^{-1} with the power of 300 mW at the sample surface.

^{31}P MAS NMR spectra were measured on a BRUKER ASX100 spectrometer with a 4 mm probe. The spinning speed was 12.5 kHz. The pulse length was 1.2 µs (pi/4), and the recycle delay was 20 s which was sufficient to enable relaxation at this field strength. ^{11}B MAS NMR spectra were measured on a BRUKER Avance 400 spectrometer with a 4 mm probe. The spinning speed was 12.5 kHz. A rotorsynchronized echo was used with selective pulse lengths of 20 µs and 40 µs for the first and the second pulse, with 10 s recycling delay. The Larmor frequencies were 40.5 MHz and 128.4 MHz for ^{31}P and ^{11}B, respectively. The chemical shifts of ^{11}B nuclei are given relative to BPO$_4$ at −3.6 ppm, those of ^{31}P are relative to 85% H$_3$PO$_4$ at 0 ppm.

Results and discussion

Glass properties

Three compositional series of borophosphate glasses xLi$_2$O–(50−x)ZnO–50P$_2$O$_5$ and xLi$_2$O–(50−x)ZnO–10B$_2$O$_3$–40P$_2$O$_5$ and xLi$_2$O–(50−x)ZnO–20B$_2$O$_3$–30P$_2$O$_5$ with x = 0, 10, 20, 30, 40 and 50 mol% Li$_2$O were synthesized and studied. All the prepared glasses were transparent and homogeneous.

The values of the glass density, ρ, for all series of glasses are given in Table 1. As can be seen from this table, the density of the studied glasses decreases with increasing content of lithium oxide in all series of glasses. The observed decrease is almost linear in borophosphate series, while in metaphosphate series the decrease in ρ is small within the region of 0–20 mol% Li$_2$O and at higher Li$_2$O content the decrease is similar to borophosphate series. The reason for this decrease is smaller atomic weight of Li$_2$O (29.88) in comparison with ZnO (81.39).

The molar volume, V_M, in all series of glasses (see Table 1) slightly decreases with increasing Li$_2$O content

Table 1 Composition, density (ρ), molar volume (V_M) and thermal expansion coefficient (α) of Li_2O–ZnO–B_2O_3–P_2O_5 glasses

Glass composition (mol%)				$\rho \pm 0.05$	V_M	$\alpha \pm 1$
Li_2O	ZnO	B_2O_3	P_2O_5	(g cm^{-3})	(cm^3)	(ppm K^{-1})
0	50	0	50	2.85	39.2	10.1
10	40	0	50	2.83	37.6	14.3
20	30	0	50	2.76	36.7	17.0
30	20	0	50	2.64	36.5	18.6
40	10	0	50	2.50	36.4	19.5
50	0	0	50	2.35	36.6	20.0
0	50	10	40	3.10	33.7	8.8
10	40	10	40	3.00	33.0	12.2
20	30	10	40	2.89	32.6	14.0
30	20	10	40	2.73	32.6	15.8
40	10	10	40	2.57	32.6	17.5
50	0	10	40	2.41	32.7	18.0
0	50	20	30	3.27	29.7	6.3
10	40	20	30	3.12	29.5	10.5
20	30	20	30	2.96	29.4	12.5
30	20	20	30	2.79	29.3	13.5
40	10	20	30	2.62	29.2	15.2
50	0	20	30	2.45	29.2	15.5

within the concentration region of $x = 0$–20 mol% Li_2O as the covalent Zn–O bonds are replaced by more ionic Li^+–O^- bonds. At higher Li_2O concentrations V_M remains almost unchanged, which we assume to be associated with the decisive role of the anionic network, which reached a minimum and the small Li^+ ions do not affect the total molar volume which is determined by the anionic network.

The values of glass transition temperature, T_g, of Li–Zn borophosphate glasses are shown in Fig. 1, and their thermal expansion coefficient α is given in Table 1. The compositional dependences of the glass transition temperature (Fig. 1) show an unmonotonous behaviour, which is most pronounced in the metaphosphate glass series, where the value of T_g reveals a minimum at 20 mol% Li_2O. Such a behaviour of Zn–Li metaphosphate glasses is similar to the mixed alkali effect observed e.g. in mixed lithium–sodium metaphosphate glasses, where the minimum of T_g was observed for the equimolar ratio of Li_2O and Na_2O [13]. In the borophosphate series we can see a significant decrease of T_g by about 100°C within the concentration region of 0–20 mol% Li_2O, while within the regions of 20–50 mol% Li_2O the changes in T_g are much smaller. The explanation of the dependencies in the borophosphate glass series is analogous to V_M, i.e. the first sharp decrease is due to the changing character of M–O bonds from covalent to ionic interaction accompanied by a decrease in the bonding forces inside the structural network. In the Li_2O-rich region the strength of the anionic network plays the decisive role in the values of $T_{g.}$

The thermal expansion coefficient (see Table 1) for all glass series increases with increasing Li_2O content and decreases with increasing B_2O_3 content. The observed increase of α with the replacement of ZnO by Li_2O gives evidence for the increasing ionicity of bonds in the glass structure. Higher bond ionicity results in a higher degree of asymmetry of the Condon–Morse potential energy curve [14] and therefore the values of α with increasing ionicity of M–O bonds increase.

The chemical durability of borophosphate glasses is higher than at the metaphosphate glass series. The results of the measurement of the conductivity of the water solution (κ) obtained after 60 min interaction of glass powder with distilled water are shown on Fig. 2. The obtained dependences show that mixed Li–Zn borophosphate glasses reveal relatively high chemical durability within the composition region of 0–30 mol% Li_2O and their chemical stability is substantially higher than that of metaphosphate glasses. The measurement of the dissolution rate of borophosphate glasses with $x = 0$–30 mol% Li_2O gave the

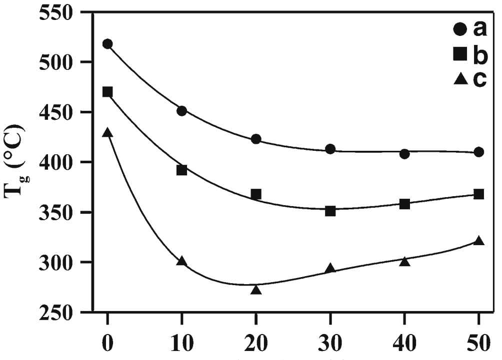

Fig. 1 Compositional dependence of the glass transition temperature, T_g, of the glass series xLi_2O–$(50-x)$ZnO–$50P_2O_5$ (**a**), xLi_2O–(50−x)ZnO–$10B_2O_3$–$40P_2O_5$ (**b**) and xLi_2O–$(50-x)$ZnO–$20B_2O_3$–$30P_2O_5$ (**c**). The errors in the data points are comparable to the size of the data points

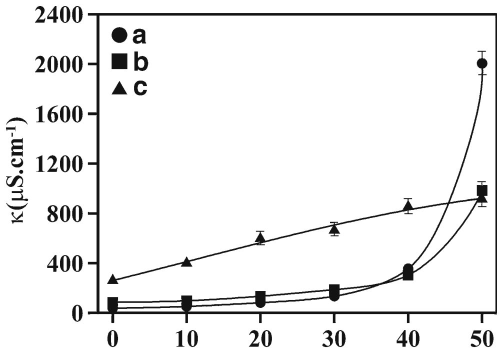

Fig. 2 Compositional dependence of conductivity, κ, of water extracts in the glass series xLi_2O–$(50-x)$ZnO–$50P_2O_5$ (**a**), xLi_2O–$(50-x)$ZnO–$10B_2O_3$–$40P_2O_5$ (**b**) and xLi_2O–$(50-x)$ZnO–$20B_2O_3$–$30P_2O_5$ (**c**). The errors in the values of κ under 400 μS cm^{-1} are smaller than the data points

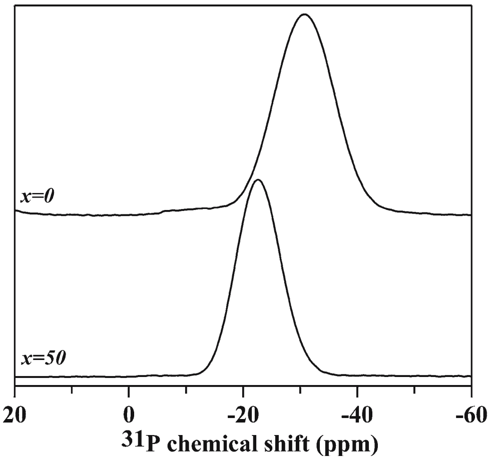

Fig. 3 ^{31}P MAS NMR spectra of the glasses $50ZnO–50P_2O_5$ ($x = 0$) and $50Li_2O–50P_2O_5$ ($x = 50$)

values 6.1×10^{-6} to 6.7×10^{-7} g cm^{-2} min^{-1}. Li-rich glasses have poor chemical durability both in metaphosphate and borophosphate glass series.

Spectral studies

Metaphosphate glasses

The ^{31}P MAS NMR spectra of the $50ZnO–50P_2O_5$ and $50Li_2O–50P_2O_5$ glasses are presented in Fig. 3. Both spectra reveal one broad signal with the maximum at −31 ppm for $Zn(PO_3)_2$ and −23 ppm for $LiPO_3$ corresponding to the presence of Q^2 units in the glass structure [15]. The determined values of the chemical shift are in agreement with the literature data for glassy $Zn(PO_3)_2$ [16] and $LiPO_3$ [17]. The change in the value of the chemical shift is dependent on the electrostatic field strength of the cation [18] and thus the shielding on phosphorus at the Zn metaphosphate is greater than at the Li metaphosphate. Raman spectra of $50ZnO–50P_2O_5$ and $50Li_2O–50P_2O_5$ glasses are given in Fig. 4. The positions of the maxima of the dominant band of symmetrical stretching vibrations of non-bridging oxygen atoms on Q^2 units, $\nu_s(PO_2)$, are in a good agreement with the literature data [19], as well as the positions of the second strong band of vibrations of bridging oxygen atoms connecting Q^2 units, ν_s(P–O–P). Both spectra are very similar, because the structure of Zn and Li metaphosphate glasses is the same, consisting of long metaphosphate chains composed of Q^2 units with cations compensating the charge on non-bridging oxygen atoms.

Borophosphate glasses with 10 mol% B_2O_3

The ^{31}P MAS NMR spectra of three glasses from the borophosphate series $xLi_2O–(50−x)ZnO–10B_2O_3–40P_2O_5$ are presented in Fig. 5. The spectrum of pure zinc borophosphate glass of the composition $50ZnO–10B_2O_3–40P_2O_5$ (Fig. 5) reveals one broad signal with the main maximum at $\delta = −25.3$ ppm and a shoulder at −8 ppm. With increasing Li_2O content, the main signal from −25.3 ppm shifts downfield to −17.4 ppm at the glass with 30 mol% Li_2O and to −14.9 ppm at the glass with 50 mol% Li_2O. Also the shoulder shifts with composition from −8 ppm up to −3.7 ppm at the glass with 50 mol% Li_2O. The position of the dominant signal lies within the region characteristic of Q^2 units in phosphate-based glasses [15] and its downfield shift with increasing Li_2O content is in agreement with smaller electrostatic field strength of Li^+ ions in comparison to Zn^{2+} ions [18]. More ionic character of M–O bonds in Li-rich borophosphate glasses results also in a smaller width of the observed NMR signal in Li-rich glasses. The smaller band on the downfield site of the dominant signal lies within the range characteristic of the Q^1 units [15] and its position is also influenced by the electrostatic field strength of the cation. Nevertheless, recent studies of Zeyer et al. [20] showed that there is a high concentration of P–O–B bonds even in the glasses of this

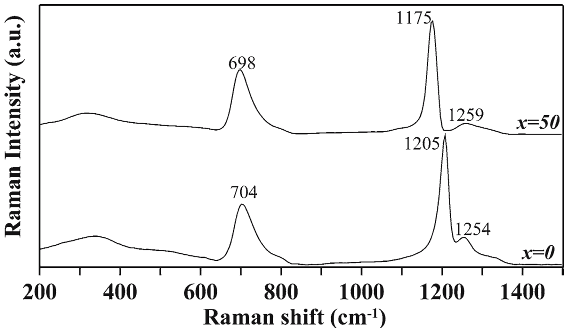

Fig. 4 Raman spectra of the glasses $50ZnO–50P_2O_5$ ($x = 0$) and $50Li_2O–50P_2O_5$ ($x = 50$)

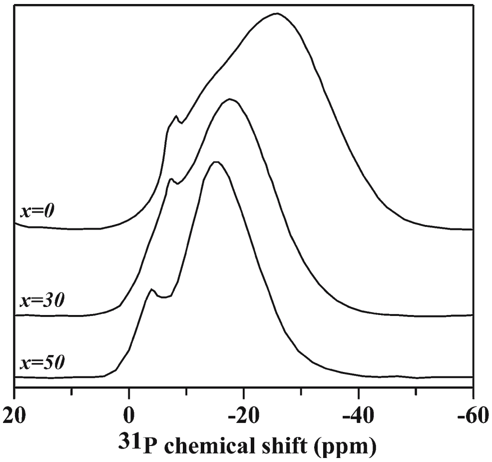

Fig. 5 ^{31}P MAS NMR spectra of the glass series $xLi_2O–(50–x)ZnO–10B_2O_3–40P_2O_5$

series and thus the main band could be characteristic of PO_4 groups bonded to BO_4 groups rather than Q^2 units with two non-bridging oxygen atoms.

The ^{11}B MAS NMR spectra of the glass series $x\text{Li}_2\text{O}–(50-x)\text{ZnO}–10\text{B}_2\text{O}_3–40\text{P}_2\text{O}_5$ are presented in Fig. 6. The spectra of the this series of glasses reveal only one NMR signal characteristic of the presence of only BO_4 units, which shifts from −3.8 ppm to −2.6 ppm with increasing Li_2O content.

The Raman spectra of the glass series $x\text{Li}_2\text{O}–(50-x)\text{ZnO}–10\text{B}_2\text{O}_3–40\text{P}_2\text{O}_5$ are shown in Fig. 7. In the high-frequency region of the Raman spectrum of the pure Zn borophosphate glass, there is one strong broad band with the maximum at 1169 cm^{-1}. With the replacement of ZnO by Li_2O, maximum of this band shifts to lower frequencies up to 1134 cm^{-1} at the $50\text{Li}_2\text{O}–10\text{B}_2\text{O}_3–40\text{P}_2\text{O}_5$ glass. This band can be assigned to symmetrical stretching vibration of non-bridging oxygen atoms in Q^2 units, which prevail in the structure according to ^{31}P MAS NMR spectra. The observed shift is comparable with that found at metaphosphate glasses. In the middle-frequency region of the Raman spectra of pure zinc glass there are two medium Raman bands with maxima at 667 and 751 cm^{-1} ascribed to ν_s(B–O–P) and ν_s(P–O–P) vibrations of B–O–P bridges and P–O–P bridges in diphosphate units, respectively [21]. The ratio of the intensity of these two bands changes a little with composition, which can be due to small changes in the bond strength under the influence of different cations.

Spectral studies of the first series of Li–Zn borophosphate glasses with 10 mol% B_2O_3 showed that the glass structure is composed of PO_4 tetrahedra and BO_4 tetrahedra interconnected by P–O–B bridges. The presence of BO_3 trigonal units has not been observed in the ^{11}B MAS NMR spectra of this composition series. Smaller vibrational coupling in Li-rich borophosphate glasses results in narrower Raman bands in the high-frequency region in comparison with Zn-rich borophosphate glasses.

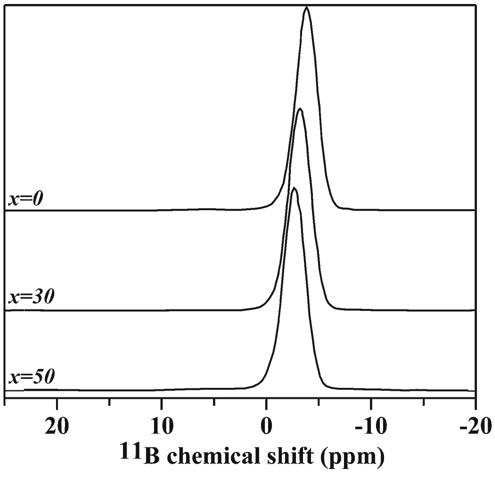

Fig. 6 ^{11}B MAS NMR spectra of the glass series $x\text{Li}_2\text{O}–(50-x)\text{ZnO}–10\text{B}_2\text{O}_3–40\text{P}_2\text{O}_5$

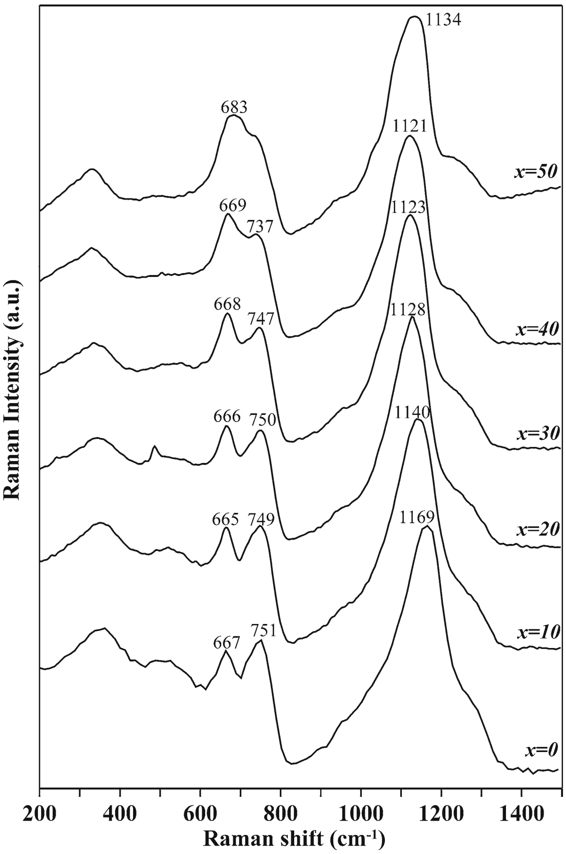

Fig. 7 Raman spectra of the glass series $x\text{Li}_2\text{O}–(50-x)\text{ZnO}–10\text{B}_2\text{O}_3–40\text{P}_2\text{O}_5$

Borophosphate glasses with 20 mol% B_2O_3

The ^{31}P MAS NMR spectra of the glass series $x\text{Li}_2\text{O}–(50-x)\text{ZnO}–20\text{B}_2\text{O}_3–30\text{P}_2\text{O}_5$ (Fig. 8) reveal similar downfield shifts as in the previous glass series. The maximum of the dominant signal shifts downfield from −14.3 ppm at the $50\text{ZnO}–20\text{B}_2\text{O}_3–30\text{P}_2\text{O}_5$ glass to −10.1 ppm at the glass with 30 mol% Li_2O down to −8.6 ppm at the glass with 50 mol% Li_2O. This broad signal was decomposed into two components with maxima at −19 ppm ($x = 0$), −12 ppm ($x = 30$) and −9 ppm ($x = 50$) for PO_4 units with P–O–B bonds and −8 ppm ($x = 0$), −3.8 ppm ($x = 30$) and −1.8 ppm ($x = 50$) for Q^1-type units. The integration of the area of both corresponding components shows on a decreasing amount of Q^1 units from about 36% to 30% and 24% at the glasses with 0, 30 and 50 mol% Li_2O, respectively in the glass series $x\text{Li}_2\text{O}–(50-x)\text{ZnO}–20\text{B}_2\text{O}_3–30\text{P}_2\text{O}_5$.

The ^{11}B MAS NMR spectra $x\text{Li}_2\text{O}–(50-x)\text{ZnO}–20\text{B}_2\text{O}_3–30\text{P}_2\text{O}_5$ are presented in Fig. 9. Contrary to the first glass

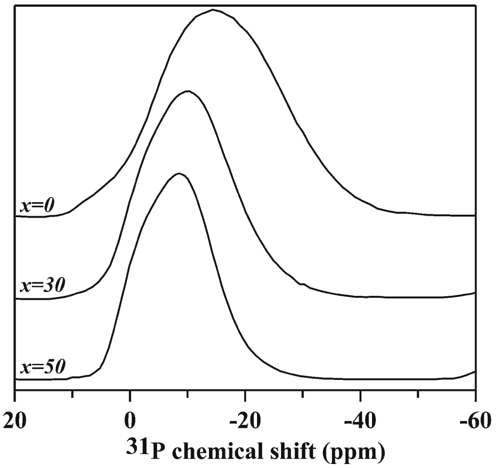

Fig. 8 ^{31}P MAS NMR spectra of the glass series xLi$_2$O–(50−x)ZnO–20B$_2$O$_3$–30P$_2$O$_5$

series, the ^{11}B MAS NMR spectrum of the pure Zn borophosphate glass composition consists of two BO$_4$ peaks with chemical shifts at $\delta = -3.4$ ppm and $\delta = -1.5$ ppm, which are assigned to B(OP)$_4$ and B(OP)$_3$(OB), respectively [22]. ^{11}B MAS NMR spectra also show a small amount of BO$_3$ units revealed by a small asymmetric signal on the left side of the BO$_4$ resonance, which is due to a second order quadrupolar effect not removed by the MAS. With increasing Li$_2$O the intensity of the higher peak decreases and on the NMR spectrum of the 50Li$_2$O–20B$_2$O$_3$–30P$_2$O$_5$ glass only the second peak is present. These changes in the signal of BO$_4$ units are accompanied by a decrease in the intensity of the band characteristic of BO$_3$ units. The decomposition of the NMR signal shows on a decrease in the number of BO$_3$ units from about 30% at the pure Zn-glass to about 12% at the pure Li-glass. It means also that the number of BO$_4$ units in the Li-glass is higher than in the corresponding Zn-glass.

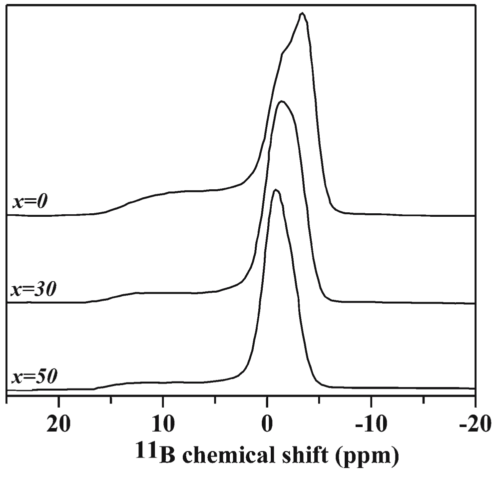

Fig. 9 ^{11}B MAS NMR spectra of the glass series xLi$_2$O–(50−x)ZnO–20B$_2$O$_3$–30P$_2$O$_5$

The Raman spectra of the glass series xLi$_2$O–(50−x)ZnO–20B$_2$O$_3$–30P$_2$O$_5$ are shown in Fig. 10. The dominant vibrational band in the pure zinc borophosphate glass is very broad, having a maximum at 1083 cm^{-1}, which splits into two strong bands of 1020 cm^{-1} and 1101 cm^{-1} with increasing Li$_2$O content. On the Raman spectrum of pure zinc glass there is also a medium band with a maximum at 748 cm^{-1}, the position of which corresponds to the stretching vibration of bridging oxygen atoms in diphosphate units. With increasing Li$_2$O content we can observe an increase in the strength of the band 655 cm^{-1} assigned to P–O–B bridges.

Results of spectral measurements in the glass series of xLi$_2$O–(50−x)ZnO–20B$_2$O$_3$–30P$_2$O$_5$ revealed interesting changes in structure of these glasses. The most significant is the information obtained from ^{11}B MAS NMR spectra, showing the decreasing number of BO$_3$ groups with increasing Li$_2$O content. We assume that this effect can be assigned to different bonding in Zn-rich and Li-rich glasses. More covalent Zn–O bonds are replaced by a weaker Li$^+$...O^{2-} interaction and free oxygen atoms support BO$_3$ to BO$_4$ conversion. Moreover, according to recent study [22] BO$_3$ units are bonded in borophosphate glasses exclusively to BO$_4$ units via B$^{(4)}$–O–B$^{(3)}$ bridges. Thus a transforma-

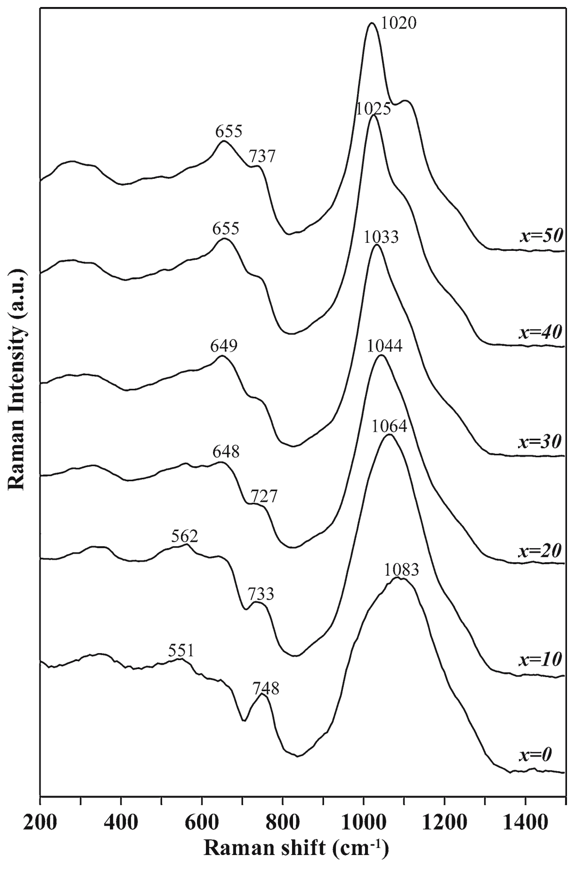

Fig. 10 Raman spectra of the glass series xLi$_2$O–(50−x)ZnO–20B$_2$O$_3$–30P$_2$O$_5$

tion of BO_3 to BO_4 units is accompanied by increasing amount of P–O–B bonds which is confirmed by changes in the Raman spectra in their middle-frequency part.

Conclusion

Study of the properties of mixed lithium–zinc borophosphate glasses revealed that the replacement of ZnO by Li_2O leads to some changes in the properties and structure of these glasses. A higher ionicity of bonds between cations and the anionic network in the Li-rich glasses is associated with a decrease in the strength of bonding interactions in the structural network. Weakening of chemical bonds in the network results in a decrease in the glass transformation temperature and the chemical durability of lithium-rich borophosphate glasses. The observed structural changes in both borophosphate glass series are associated with different behaviour of ZnO and Li_2O in the glasses. Zinc oxide belongs to intermediate oxides and therefore it is able to enter structural network and form covalent Zn–O–P bonds. Li_2O is a typical modifying oxide and thus it gives off oxygen atoms to the structural network forming Li^+ ions and the interaction of Li^+ ions with glass network is weaker. Li^+ ions are able to move inside the network, which is the base of the application of Li-glasses in solid electrolytes.

Acknowledgement The Czech authors are grateful for the financial support of the Grant Agency of Czech Republic (Grant No. 104/04/0711) and from the research project No. 0021627501 of the Ministry of Education of Czech Republic.

References

1. Malugani J, Wasniewski A, Doreaus M, Robert G, Al Rikabi A (1978) Mater Res Bull 15:427
2. Pradel A, Pagnier T, Ribes M (1985) Solid State Ionics 17:147
3. Martin SW, Angell CA (1986) J Non-Cryst Solids 83:185
4. Tatsumisago M, Kowada ZY, Minami T (1988) Phys Chem Glasses 29:63
5. Magistris A, Chiodelli O, Villa M (1985) J Power Source 14:87
6. Scagliotti M, Villa M, Chiodelli G (1987) J Non-Cryst Solids 93:350
7. Jin Y, Chen X, Huang X (1989) J Non-Cryst Solids 112:147
8. Scagliotti M, Villa M, Chiodelli G (1987) J Non-Cryst Solids 94:101
9. Tian F, Pan L (1989) J Non-Cryst Solids 112:142
10. Brow RK, Tallant DR (1997) J Non-Cryst Solids 222:396
11. Koudelka L, Mošner P, Večeřa M (2000) J Mater Sci 35:5593
12. Koudelka L, Mošner P (2000) Mater Lett 42:194
13. Green PF, Brow RK, Hudgens JJ (1998) J Chem Phys 109:7907
14. Shelby JE (1997) Introduction to glass science and technology. Royal Society of Chemistry, Cambridge, p 147
15. Mustarelli P (1999) Phosphorus Res Bull 10:25
16. Brow RK, Tallant DR, Myers ST, Phifer CC (1995) J. Non-Cryst Solids 191:45
17. van Wüllen L, Eckert H, Schwering G (2000) Chem. Mater. 12:1840
18. Montagne L, Palavit G, Delaval R (1997) J. Non-Cryst Solids 215:1
19. Nelson C, Exarhos G.J (1979) J Chem Phys 71:2739
20. Zeyer-Düsterer M, Montagne L, Palavit G, Jäger CH (2005) Solid State Nucl Magn Reson 27:50
21. Koudelka L, Mošner P, Zeyer M, Jäger C (2002) Phys Chem Glasses 43C:102
22. Elbers S, Strojek W, Koudelka L, Eckert H (2005) Solid State Nucl Magn Reson 27:65